Langmuir

ARTICLE

pubs.acs.org/Langmuir

# The Role Played by Salts in the Formation of SBA-15, an in Situ Small-Angle X-ray Scattering/Diffraction Study

C. V. Teixeira,[†,‡,⊥] H. Amenitsch,[§] P. Linton,[∥] M. Lindén,[‡] and V. Alfredsson[*,#,∥]

[†]Universitad Autonoma de Barcelona, Facultad de Medicina, Unidad de Biofisica-Cerdanyola del Valles, 08193, Spain

[‡]Center for Functional Materials, Department of Physical Chemistry, Åbo Akademi University, Porthansgatan 3-5, FI-20500 Turku, Finland

[§]Institute of Biophysics and Nanosystems Research, Austrian Academy of Sciences, Schmiedlstrasse 6, A-8042 Graz, Austria

[∥]Physical Chemistry, Box 124, Lund University, SE-221 00 Lund, Sweden

[⊥]Institute of Physics, Universidade Federal do Rio Grande do Sul, Caixa Postal 15051, CEP 91501-970, Porto Alegre, RS, Brazil

Supporting Information

**ABSTRACT:** The influence of salts (NaCl, NaBr, and NaI) on the formation of mesoporous silica SBA-15 was studied in situ by small-angle X-ray scattering and diffraction. Pluronic P104 was used as structure director. The micellar properties and the dynamics of formation were clearly dependent on the presence of salt. It was also shown that the kinetics of mesophase formation, the initial value of the cell parameters, and the extent of long-range order were all influenced by salt additions. The observations are explained to primarily originate from the influence of the anions on the ethylene oxide part of the polymer, i.e., the corona region of the Pluronic micelles. Two effects are identified: a general ion effect causing dehydration of the ethylene oxide part and consequently inducing micellar growth, and a specific ion effect that counterbalances this. The study provides the basis for understanding the means by which addition of simple Na-salts influence the formation of mesoscopically ordered silicas synthesized using nonionic surfactants as structure directors, hence advancing the knowledge base toward a more rational design of mesoporous materials.

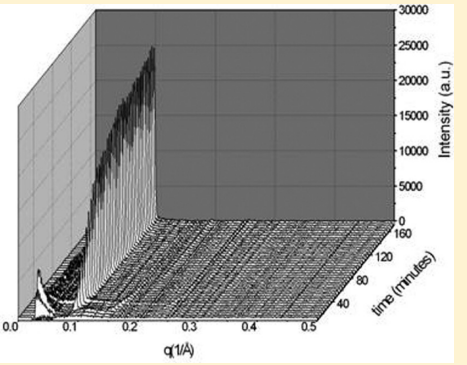


## INTRODUCTION

Almost two decades of intensive research on ordered mesoporous materials have resulted in a large abundance of materials with varying properties with respect to structure, chemical composition, and particle morphology. Even so, new materials, made by novel synthetic approaches or by using unexploited reagents, continue to appear in the scientific literature. The understanding of the processes involved in forming these highly ordered, yet atomically amorphous, materials still lags behind, although in the last five years or so, an increased interest in this topic has emerged. The aim of this paper is to further the understanding in this field by investigating the dynamics of formation of SBA-15[1] as a function of electrolyte additions. The incentive for studying electrolyte additions stems from the fact that simple salts have been observed to have a great influence on the mesoporous material formed.[2−9]

Synthesis of mesoporous silica materials can be performed with substantial variations of the synthesis conditions. The amphiphilic molecule present in the synthesis is essential for directing the formation toward a particular structure. Amphiphiles that are versatile in this respect are block copolymers, in particular, the family of Pluronic triblock copolymers consisting of a central polypropylene oxide block $(PO)_x$ confined between two polyethylene oxide blocks $(EO)_y$.[10] In an aqueous solution, the Pluronic polymer typically forms micelles consisting of a hydrophobic core, made up essentially from the PO part, and a hydrophilic corona where most of the EO is located.[11] Water forms an integral part of the corona but also penetrates to a certain extent into the micellar core. The size of the PO block as well as the EO blocks can be varied, allowing tuning of the amphiphilic properties of the polymers.[10] The characteristics of the polymer can also be controlled by the properties of the solvent, e.g., by additions of simple electrolytes[12] or alcohols,[13] or as a result of a temperature change.[14] It should be noted that the polymers have an inverse effect on solubility with temperature, leading to immiscibility (clouding) at elevated temperature, as both the EO and PO blocks become more hydropohobic with increasing temperature.[10]

It is well-known that electrolytes affect the properties of Pluronic polymers. The influence of electrolytes on the critical micellization temperature (cmt) as well as the phase separation, or cloud point (cp), for aqueous solution of Pluronic block copolymers[12] has been studied by differential scanning calorimetry. It was concluded that both the cmt and the cp values

**Received:** November 3, 2010
**Revised:** April 10, 2011
**Published:** May 06, 2011

depended on the type of anion and cation, respectively. For instance, for a selection of anions it was shown that the influence on both parameters (cp and cmt) decreased in the order $Cl^- > Br^- > I^-$. Kabalnov et al.[15] explained the analogous effect observed in a system of a nonionic microemulsion to have an interfacial origin, due to the anions being either adsorbed to or depleted from the polyethylene oxide chain region of the nonionic surfactant micelles. The authors argue that large polarizable anions, such as $I^-$, adsorb in the EO part whereas smaller anions, such as $Cl^-$ and $Br^-$, are depleted from this part. This depletion leads to dehydration of the EO part, as an effect of an osmotic equilibrium.

The anions of the Hofmeister series are ordered in terms of their effect on protein solubility, as $SO_4^{2-}$, $HPO_4^{2-}$, $OH^-$, $F^-$, $HCOO^-$, $CH_3COO^-$, $Cl^-$, $Br^-$, $NO_3^-$, $I^-$, $SCN^-$, $ClCO^{4-}$. $Cl^-$ represents a borderline case, where the anions on its left are responsible for reducing the proteins solubility (salting out), whereas the anions on its right increase the proteins solubility (salting-in).[16] $Cl^-$, although on the borderline, is typically known to cause the salting-out effect. $Br^-$ is very close to $Cl^-$ and hence has a quite similar effect, however, tending to the side of the salting-in salts.

The now classical mesoporous silica structure SBA-15,[1] defined by the plane group *p6m*, is synthesized with Pluronic polymers, with P123 being the most commonly used structure director. We, however, use P104, as this polymer, to the best of our knowledge, exclusively promotes the *p6m* structure, whereas P123 can give rise to other structures under appropriate conditions.[7,17] Typically, the synthesis is performed under strongly acidic conditions (pH < 0) with a silicon alkoxide as the silica source. The material resulting from the synthesis can be controlled by variation of the synthesis conditions, for instance, by adjusting parameters such as temperature[18] and electrolyte concentration[4,19] even though the ionic strength of the solution is normally high already due to the high mineral acid concentration. These parameters are known, as mentioned above, to also affect the phase behavior of the amphiphilic structure director.

Formation of SBA-15, as well as related Pluronic-directed mesoporous silica materials, has been studied by a range of techniques.[20−27] A useful technique for this type of investigation, which has previously been used by us[28−30] as well as by others,[31−33] is in situ small-angle X-ray scattering (SAXS). This technique can provide information regarding the micelles as well as the emerging mesoscopically ordered material. There are at present different views on the sequence of events that lead to the formation of SBA-15. A complication in this respect is the fact that the systems investigated are not identical but differ regarding reagents and synthesis temperature.

In brief, our[24,28,30,34] understanding of the formation of SBA-15 (under strongly acidic conditions (1.6 M HCl) where the silica network is expected to have a cationic charge) is as follows: siliceous species such as oligomers in solution associate with the micellar corona, i.e., the EO part of the Pluronic polymer, likely as a result of hydrophobic interactions.[24] This association is faster if silica has condensed somewhat prior to addition to the Pluronic solution.[35] Eventually, phase separation occurs where droplets, or flocs, of a concentrated phase, consisting of aggregates of siliceous micelles, appear in the dilute aqueous solution. With time, the micelles in the flocs rearrange and grow into elongated micelles that pack in a hexagonal array, and hence, the mesoscopically ordered particles are obtained. The time scale for this process, depending on the specific synthesis conditions, is on the order of 10−30 min. Recently, we realized that particles are not the result of a typical nucleation and growth process, but other steps can occur that have an impact on the particle size and morphology.[30,34,36] However, these steps do not seem to affect the mesoscopic order. It was also observed that the flocs nucleate (as observed with UV−vis spectroscopy) approximately five minutes prior to the first appearance of the hexagonal phase[30] and prior to an observable precipitation. Hence, precipitation does not indicate formation of particles but is the result of an unspecific aggregation of several particles (single (meso)crystals). The lag time between formation of flocs and appearance of the hexagonal phase is expected to vary considerably depending on the synthesis conditions.

Simple electrolytes have been shown to influence the synthesis and the resulting material when Pluronic polymers are used as structure directors. Here, without the intent of giving an extensive inventory, we mention a few examples, in which electrolytes have been shown to influence Pluronic assisted syntheses. It has been shown that addition of electrolytes facilitate synthesis performed at lower temperatures.[19] Addition of NaI can also be used to redirect a SBA-15 synthesis to the bicontinuous Ia3d structure.[7] Tang et al.[4] showed that the outcome of the synthesis of KIT-6[17] was dependent on the anions present in the reagent solution. Not only do electrolytes influence the structural properties, but particle morphology and porosity are also strongly dependent on the presence of inorganic salts.[2,8,9,36−38] Recently, the location of nitrates with respect to the micelles was investigated.[39] It was shown that the siliceous species outnumber the nitrates in the micellar corona and that the structure formed depends on a delicate interplay between the anions present in the reagent solution.

Thus, electrolytes can clearly be used to control the Pluronic assisted mesoporous silica synthesis, although the fundamental knowledge of the mechanisms responsible is still lacking. The incentive for this work is to understand the dynamics of formation of SBA-15 with respect to addition of a series of salts. While conserving the cation ($Na^+$), the influence of three anions ($Cl^-$, $Br^-$, and $I^-$) known to have different salting-in/out properties was investigated. It should be noted that in all the syntheses 1.6 M HCl is present; thus, in all cases there is a high background concentration of chloride ions. Hence, there will always be a competition between the $Cl^-$ ions already present and the $Br^-$ and $I^-$ ions added. We have studied the dynamics of the syntheses as a function of time with small-angle X-ray scattering/diffraction (SAXS/SAXD).

The dynamics of formation provides fundamental understanding for a number of material charcteristics, for instance, particle size and morphology. The embryonic particles (or flocs, see above) arise as droplet nuclei are formed and then grow in size as long as there are reactants available.[34] Typically, a fast nucleation burst results in many nuclei and leads to a large number of small and well-defined particles; a slower, more sluggish process leads to less distinct growth and particles with varying sizes/morphologies. These particle characteristics are dominated by the early stages of formation, which can be monitored by SAXS/SAXD. The porosity of the materials is closely linked to the shape of the micellar porogenes, but the hydrothermal process and the calcination process usually employed to arrive at the porous material have a large influence on the porosity of the final material, and the characteristics of the porosity cannot simply be understood from the dynamics of

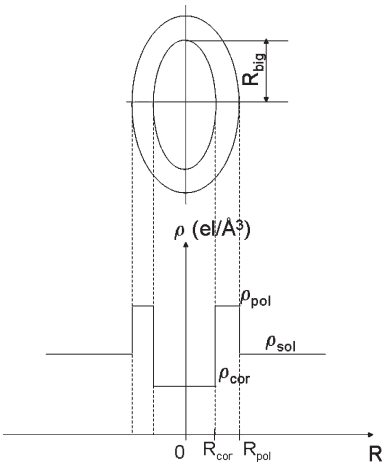


**Figure 1.** Model of micelle used for the calculation of the form factor of prolate ellipsoid. The dimensions of the micelles are $R_{cor}$= radius of the hydrophobic region in the smaller axis; $R_{pol}$ = the total radius of the micelle in the smaller axis; $R_{big}$= the hydrophobic radius in the longer axis. $\rho_{par}$ = 0.332 electrons/Å$^3$ is electron density of the PO units; $\rho_{pol}$ = electron density of the hydrophilic region, obtained from the fittings; $\rho_{sol}$ = electron density of the solvent (0.352 electrons/Å$^3$ for no salt; 0.359 electrons/Å$^3$ for 0.5 M NaCl; 0.361 electrons/Å$^3$ for 1.0 M NaCl; 0.376 electrons/Å$^3$ for 1.5 M NaCl; 0.364 electrons/Å$^3$ for 0.5 M NaBr; 0.378 electrons/Å$^3$ for 1.0 M NaBr; and 0.392 electrons/Å$^3$ for 1.5 M NaBr).

formation. Influence of the salt additions on the porosity is the topic of a separate publication.

The in situ experiments were performed at the Austrian SAXS beamline at Elettra. The salts were added prior to the onset of the synthesis (i.e., prior to addition of the silica source). Although three salts (NaCl, NaBr, and NaI) were used, only the results from two of them (NaCl and NaBr) will be discussed in more detail, as the high X-ray absorption of the iodide-containing solutions made detailed analysis of the scattering/diffraction data impossible. In the discussion, we will include some qualitative data obtained from the NaI containing synthesis. Scanning electron microscopy was used to investigate particle size/morphology of as-synthesized particles.

## EXPERIMENTAL SECTION

Pluronics P104 ($EO_{27}PO_{61}EO_{27}$) from BASF, tetraethyl orthosilicate (TEOS) from Aldrich, HCl from Merck, and NaCl, NaBr, and NaI from Aldrich were used. The syntheses were performed by weighing 0.481 g of P104 in 18.75 g solution of 1.6 M HCl, resulting in 2.5 wt % solution of P104. NaCl, NaBr, and NaI were added to different samples at the concentrations of 0.5, 1.0, and 1.5 M. One sample without addition of salt was also studied. All reactions were investigated at a fixed temperature of 45 °C. The reaction was initiated by adding 1.0 g TEOS to the solution under vigorous stirring.

The reaction was carried out in a batch reactor connected to a 1.5 mm flowthrough X-ray capillary through which the sample was pumped. The solution was then pumped back to the batch reactor (pumping rate 70 mL/min), forming a closed-loop system. The tubings were thermally insulated. The setup has been described previously.[40] Both the reactor and the capillary were thermostatted to the desired temperature (45 °C). The time-resolved measurements were performed at the Austrian SAXS beamline of the 2 GeV electron storage ring Elettra (Trieste, Italy).[41] The data were collected with a position-sensitive Gabriel detector and the photon energy was 8 KeV. The detector was calibrated with silver behenate (*d*-spacing 58.38 Å).

Scanning electron micrographs were recorded with a JEOL JSM-6700. The as-synthesized materials were sputter-coated with gold prior to imaging.

**Analysis Method.** The scattering curves have been corrected for variations in the intensity of the primary beam and the background (1.6 M HCl in water plus the equivalent concentration of salt for each solution) was subtracted. The form factors of prolate ellipsoids and infinite cylinders were fitted to the curves. The form factors were calculated using a model of three different electron density levels, as illustrated in Figure 1 for an ellipsoid. The form factor of a prolate ellipsoid is given by[42]

$$P(q) = \int_0^{\pi/2} \left\{ \left(\rho_{cor} - \rho_{pol}\right)\frac{4\pi}{3} \nu R_{cor}^3 \phi\left[qR_{cor}g_1(\theta)\right] + \left(\rho_{pol} - \rho_{sol}\right)\frac{4\pi}{3} R_{pol}^2 (\nu R_{cor} + t)\phi\left[qR_{pol}g_2(\theta)\right] \right\}^2 \cos\theta \, d\theta \quad (1)$$

where $R_{cor}$ is the radius of the smaller axis of the micelle core; $R_{pol}$ = $R_{cor} + t$ is the total radius of the smaller axis of the ellipsoid, and $t$ is the thickness of the corona.

$$\phi(u) = 3\left[(\sin u - u\cos u)/u^3\right]$$

$$g_1(\theta) = (\cos^2\theta + \nu^2 \sin^2\theta)^{1/2}$$

$$g_2(\theta) = (\cos^2\theta + \nu'^2 \sin^2\theta)^{1/2}$$

$$\nu' = (\nu R_{cor} + t)/(R_{cor} + t)$$

and $\nu$ is the axial ratio between the long and short axes of the hydrophobic part.

In the case of infinitely long cylinders, when nearly perpendicular to the scattering vector $\mathbf{q}$[43]

$$P(q) = L\frac{\pi}{q}\left[R_{cor}^2 \times \left(\rho_{cor} - \rho_{pol}\right) \times 2\frac{J_1(qR_{cor})}{qR_{cor}} + R_{pol}^2 \times \left(\rho_{pol} - \rho_{sol}\right) \times 2\frac{J_1(qR_{pol})}{qR_{pol}}\right]^2 \quad (2)$$

where $J_1$ is the Bessel function of the first order and the length $L$ of the cylinder is much larger than its radius.

The electron densities ($\rho$) are given in electrons/Å$^3$. $\rho_{cor}$ (electron density of the micellar core) was calculated from the number of electrons in a PO chain divided by its volume (0.332 electrons/Å$^3$) and kept constant in all the fitting procedures. $\rho_{sol}$ (electron density of the solvent) was calculated by considering the number of electrons of the water molecule, HCl, and salt (values presented in Figure 1) and was kept constant for the respective fittings but different for each synthesis condition. $\rho_{pol}$ (electron density of the corona region) was initially calculated from the number of electrons per Å$^3$ in a EO chain, and used as a starting value, but left as a free parameter. $R_{cor}$, $R_{pol}$, and $\nu$ (axial ratio between the long and short axes of the hydrophobic part for ellipsoids) were free parameters, where $R_{pol}$ was constrained by the cell parameter at the moment of appearance of the first Bragg reflection as an absolute limit for the maximum diameter for the cross section of the micelles. The fitted $R_{cor}$ and $R_{pol}$ were constrained to be the same for ellipsoids and infinite cylinders for the same fitted curve. The curves before the appearance of the Bragg reflections were modeled only by the micellar form factor. After the appearance of the ordered phase, the peak position, full-width at half-maximum (fwhm), and integrated intensity were determined by fitting of Lorentzian functions.


dx.doi.org/10.1021/la1043798 |*Langmuir* 2011, 27, 7121–7131

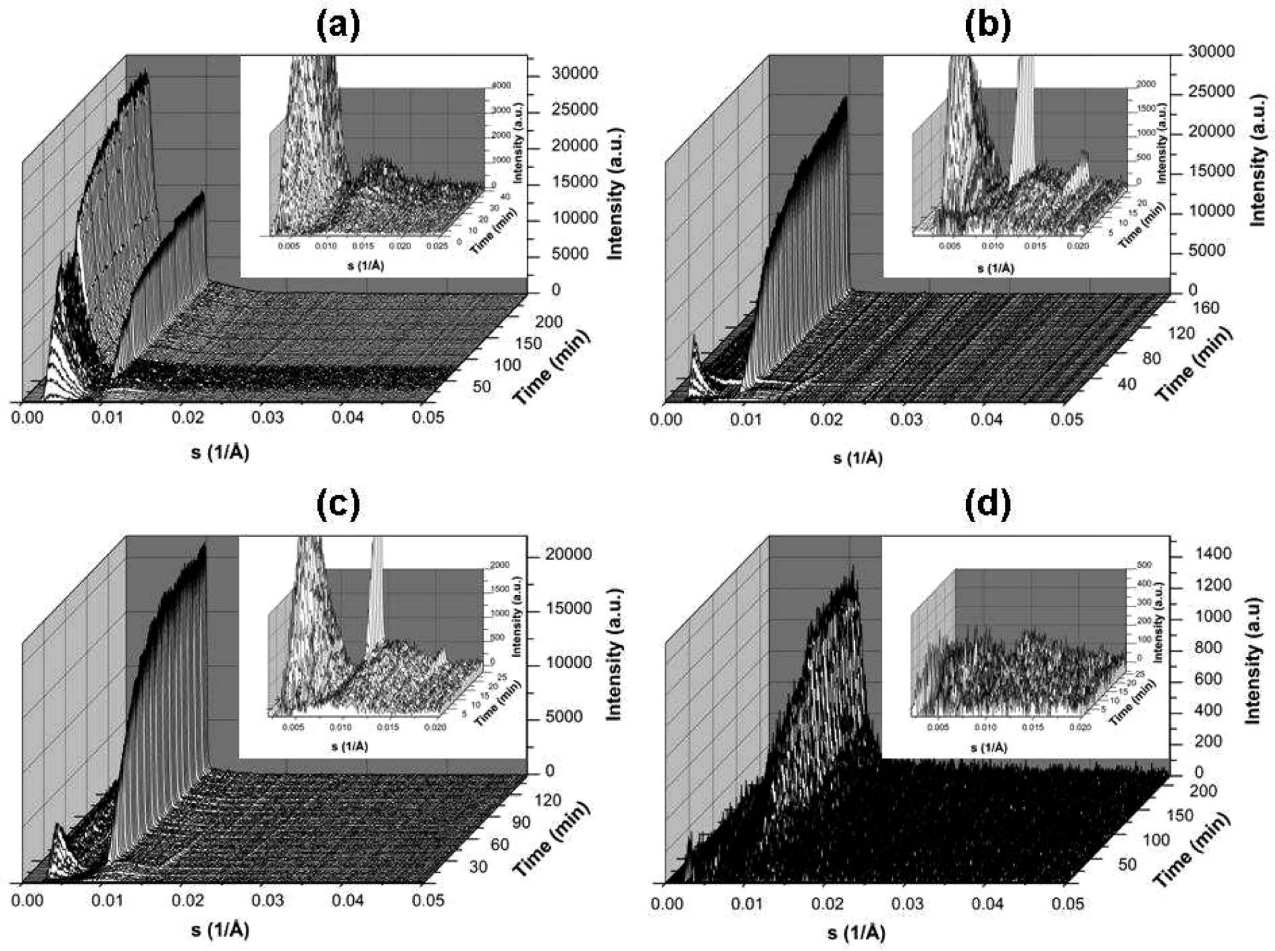


**Figure 2.** Time-resolved SAXS patterns of the synthesis of SBA-15 with Pluronic P104 as structure promoter with (a) no salt; (b) 1.0 M NaCl; (c) 1.0 M NaBr; (d) 1.0 M NaI. The appearance of the Bragg reflections marks the point in time when the hexagonal (*p6m*) phase first occurs. This time is dependent on the electrolyte. Prior to the arrival of the Bragg reflections, micellar scattering is observed as oscillations at very low angles (not observed for NaI containing synthesis due to the large background scattering from iodine). With time, the intensity of these oscillations increases as a consequence of the association of siliceous species to the micellar corona. The insets show an enlargement of the initial stages of formation, i.e., the evolution of the form factor oscillations in detail.

## RESULTS

The time-resolved SAXS patterns of the formation of SBA-15 without any added salt and with 1.0 M NaCl, NaBr, and NaI are shown in Figure 2. In all cases (except for NaI where the signal-to-noise ratio was too low), a micellar form factor oscillation (manifested as wavelike oscillations at low angles) is observed prior to the occurrence of Bragg reflections characteristic of a 2D hexagonal phase. The intensity of the micellar scattering increases with time, due to the increase in the electron density in the corona region of the micelles due to adsorption of silicate species.[44] In the sample without salt, the micellar scattering is visible up to the end of the measurement time (confirming the continued presence of micelles), but in the samples containing NaBr, and especially NaCl, the micellar scattering decreases considerably in intensity after the formation of the ordered phase. The samples containing 0.5 and 1.5 M of both salts follow the same trend, as seen in Figure S1 in the Supporting Information. The time needed for formation of the ordered phase was different for each salt concentration (seen in Figure 2a–d as the different times needed for the appearance of the Bragg reflections) and different for each salt (cf. Table 1). Further, prior (ca. 5 min, but dependent on type of salt and the concentration) to the appearance of the Bragg reflections a phase separation was observed, as the samples became turbid. These general considerations immediately suggest that the addition of salt, as well as the nature of the anion, have an influence on the formation kinetics of the mesophase. In the following, we will discuss the results in more detail starting with the influence of salt on the micellar properties during the induction phase, before discussing the part concerning the formation and evolution of the ordered structure.

The micellar region of the curves was fitted using eqs 1 and 2, for ellipsoids and infinite cylinders, respectively. We did not consider it necessary to include polydispersity in our model (as polydispersity in length has negligible influence as the aggregates grow longer and the radius tend to be constant). Typically, scattering curves measured 5 and 10 min into the reaction and the scattering curve measured just prior to the appearance of Bragg reflections were fitted. It should be noted that this latter time is different for each synthesis. As the form factor of infinitely long cylinders contains the term $1/q$ (eq 2), the intensity of the scattering curve for cylinders grows very rapidly when $q$ becomes very small, and thus, the low-$q$ region


dx.doi.org/10.1021/la1043798 |*Langmuir* 2011, 27, 7121–7131

**Table 1. Parameters Obtained from the Suitable Fittings of Form Factors to the Experimental Curves, Time of Formation of Hexagonal Phase, Time of Precipitation, and the Cell Parameter when the Hexagonal Phase Has Just Formed[a]**

| | | | | | . | | electron density ($\rho$) of the corona region (electrons/Å$^3$) | | | | |
|---|---|---|---|---|---|---|---|---|---|---|---|
| sample | time (min) | $R_{core}$ (Á) (±1) | corona thickness (Á) (±1) | $v$ axial ratio | $\chi_{red}^2$ ellipsoid | $\chi_{red}^2$ inf. cylinder | prolate ellipsoid | infinite cylinder | onset hex. phase (min) | phase sep. time (min) (±1) | cell param. onset hex phase (Å) (±2) |
| No salt | 5 | 31 | 31 | 2.2 (±1) | 6.13 | 7.57 | 0.384 (±0.004) | 0.400 (±0.001) | 38 ± 1 | 30 | 127 |
| | 10 | 31 | 31 | 4.6 (±0.1) | 10.69 | 9.40 | 0.392 (±0.001) | 0.420 (±0.002) | | | |
| | 30 | 31 | 31 | 7.3 (±0.2) | 7.08 | 5.80 | 0.406 (0.002) | 0.460 (0.003) | | | |
| 0.5 M NaCl | 5 | 34 | 31 | 8 (±1) | 13.26 | 30.97 | 0.390 (±0.008) | 0.428 (±0.001) | 24 (±0.2) | 17 | 131 |
| | 10 | 34 | 31 | 9 (±1) | 14.5 | 45.0 | 0.402 (±0.002) | 0.451 (±0.002) | | | |
| | 24 | 34 | 31 | 10.2 (±0.8) | 27.19 | 27.3 | 0.421 (±0.002) | 0.504 (±0.004) | | | |
| 1.0 M NaCl | 5 | 34 | 29 | 3.8 (±0.1) | 4.75 | 3.32 | 0.386 (±0.001) | 0.396 (±0.003) | 14 ± 1 | 10 | 134 |
| | 10 | 34 | 29 | 4.5 (±0.1) | 6.29 | 4.21 | 0.400 (±0.002) | 0.420 (±0.004) | | | |
| | 13 | 34 | 29 | 6.5 (±0.4) | 4.80 | 4.26 | 0.400(±0.003) | 0.429 (±0.003) | | | |
| 1.5 M NaCl | 5 | 38 | 26 | 5.1 (±0.2) | 10.94 | 15.8 | 0.422 (±0.001) | 0.454 (±0.004) | 8.5 (±0.2) | 5 | 140 |
| | 8 | 38 | 26 | 5.5 (0.2) | 9.37 | 40.20 | 0.435 (±0.001) | 0.483 (±0.006) | | | |
| 0.5 M NaBr | 10 | 25 | 39 | 6.1 (±0.4) | 7.07 | 4.75 | 0.390 (±0.003) | 0.409 (±0.002) | 33 ± 1 | 23 | 122 |
| | 30 | 25 | 39 | 9.0 (±0.2) | 56.94 | 15.50 | 0.403 (±0.001) | 0.450 (0.006) | | | |
| 1.0 M NaBr | 5 | 32 | 31 | 2.2 (±0.1) | 7.17 | 6.34 | 0.404 (±0.001) | 0.410 (±0.001) | 18 ± 1 | 12 | 127 |
| | 10 | 32 | 31 | 3.1 (±0.1) | 11.44 | 9.53 | 0.411 (±0.001) | 0.427 (±0.001) | | | |
| | 15 | 32 | 31 | 3.3 (±0.1) | 14.05 | 7.51 | 0.422 (±0.001) | 0.439 (±0.001) | | | |
| 1.5 M NaBr | 11 | 26 | 34 | 4.5 (±0.5) | 28.32 | 25.16 | 0.411 (±0.001) | 0.421 (±0.001) | 13 ± 1 | 6 | 123 |
| 1.0 M NaI | -- | -- | -- | -- | -- | -- | -- | -- | 26 ± 3 | 25 | 111 |

[a] The sample containing 1.5 M NaCl could not be studied at 10 min as the hexagonal phase occurred earlier. Fitting for 0.5 and 1.5 M NaBr is only to show the tendency of the curves, as these curves do not have sufficient resolution. Samples containing NaI do not present the micellar regime.



dx.doi.org/10.1021/la1043798 |*Langmuir* 2011, 27, 7121–7131

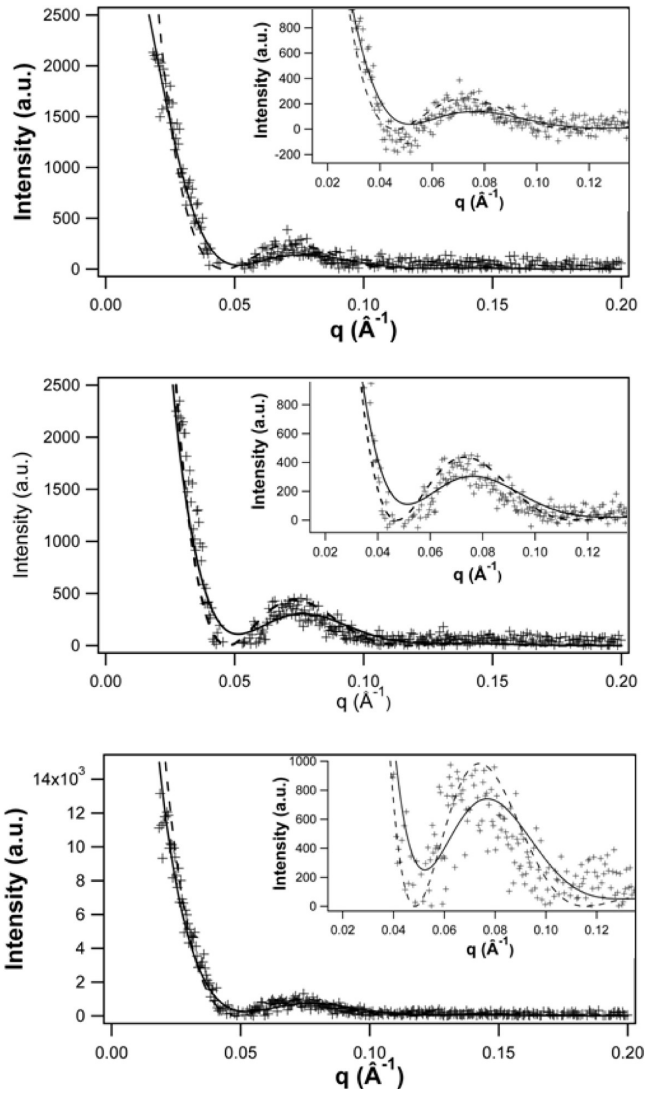


**Figure 3.** Scattering curves of P104 (no salt) in 1.6 M HCl and 1 g TEOS, along with the fitted form factors for prolate ellipsoids (—) and infinite cylinders (- - -). Top, after 5 min in the reaction; middle, 10 min in the reaction; and bottom, 30 min in the reaction, just prior to the appearance of the hexagonal phase. The parameters obtained from the fittings are presented in Table 1.

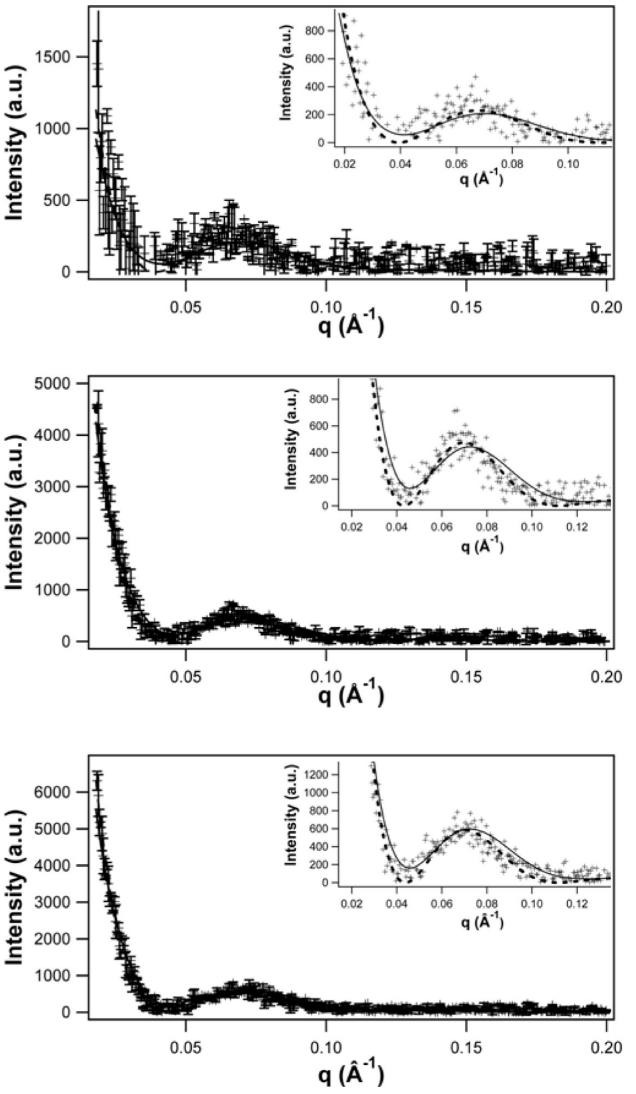


**Figure 4.** Scattering curves of P104 with 1.0 M NaCl in 1.6 M HCl and 1 g TEOS, along with the fitted form factors for prolate ellipsoids (—) and infinite cylinders (- - -). Top, after 5 min in the reaction; middle, 10 min in the reaction; and bottom, 13 min in the reaction, just prior to the appearance of the hexagonal phase. The parameters obtained from the fittings are presented in Table 1.

gives further information about the dominant shapes of the micelles. Parameters derived from the fittings together with the corresponding $\chi^2_{red}$ (see below) values are summarized in Table 1.

$\chi^2$ is defined as

$$\chi^2 \equiv \sum_{i=1}^{N} \left[ \frac{I_{exp}(q_i) - I_{mod}(q_i)}{\sigma_i} \right]^2$$

$I_{exp}$ is the experimental intensity, $I_{mod}$ the modeled intensity, and $\sigma_i$ the statistical uncertainty. The reduced $\chi^2$ is

$$\chi^2_{red} = \frac{\chi^2}{N - M}$$

with $N$ being the number of points in the curved fitted and $M$ the number of parameters fitted. $N - M$ is the degrees of freedom. An optimum $\chi^2_{red}$ value is the smallest possible value between 1 and 10. From the value of the $\chi^2_{red}$-factor, the ellipsoidal model fits better for the syntheses containing no salt and 0.5 and 1.5 M NaCl, while the infinite cylinder model gave the better fit for all other studied syntheses.

The scattering curves measured for the "no salt" sample and the corresponding fittings are shown in Figure 3 and also in log−log scale in Figure S2 of Supporting Information. The curves and fittings corresponding to 1.0 M NaCl are shown in Figure 4 (linear scale) and in Figure S3 (Supporting Information) in log−log scale. The samples with 0.5 and 1.5 M NaCl and 0.5, 1.0, and 1.5 M NaBr are shown in Supporting Information Figures S4 to S8, respectively. The insets in the figures are enlargements of the low angle region. The fitting quality was followed by the calculated $\chi^2_{red}$ values for prolate ellipsoids and infinite cylinders respectively and visual inspection of the fitted form factors to the curves. Table 1 shows the respective $\chi^2_{red}$ values for each fit.


dx.doi.org/10.1021/la1043798 |*Langmuir* 2011, 27, 7121–7131

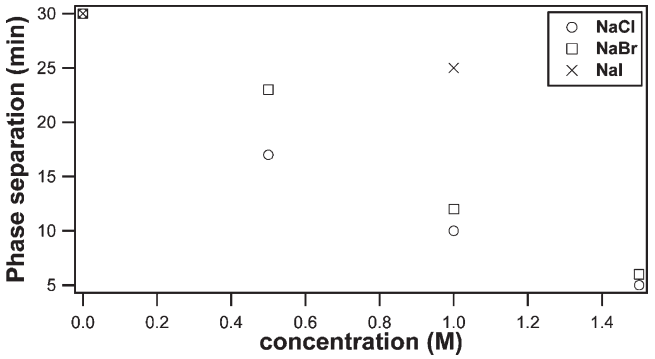


**Figure 5.** Time of phase separation, for all the syntheses studied (NaCl and NaBr at 0.5, 1.0, and 1.5 M and NaI at 1.0 M along with the synthesis performed with no salt).

At 5 min into the reactions, the $\chi^2_{red}$ values indicate that, for no salt, 0.5 M NaCl, and 1.5 M NaCl samples, the micelles are ellipsoids. Visual inspection of the curve for 1.0 M NaCl, however, shows that both shapes fit well, and therefore, there might be a mixture of both types of micelles. The samples containing NaBr was compromised by the high-background X-ray absorbance due to the high absorption of these elements at 8 keV. This was a special complication at short reaction times, where the scattering length contrast between the micelles and the solvent was low.

At 10 min into the reaction, practically all curves showed better fitting for infinite cylinders, with the exception of the sample containing 0.5 M NaCl, but this is probably due to the deeper minimum of the cylinder form factor in comparison to the experimental curve. However, for the low-$q$ slope and the first oscillation itself, a visual inspection of the curve shows that the infinite cylinder form factor is also acceptable as a good fitting, and the axial ratio of the ellipsoids are very high; thus, the micelles can be considered infinitely long, as "seen" by the X-rays. At the time of appearance of the hexagonal phase, at times higher than 10 min, all samples consist of infinitely long cylinders. However, for the sample with 1.5 M NaCl, the hexagonal phase occurs already at 8.5 min. Even if the $\chi^2_{red}$ value is better for the ellipsoidal fitting at this time, the axial ratio ($\nu$) for this curve is quite large, indicating the presence of very long micelles. It is visible in the curves that the infinite cylinder form factor fits the oscillation and the slope at low-$q$ values well (see Supporting Information Figure S5).

Generally speaking and by examining the results presented in Table 1, the micelles in all samples, with or without salt, at all concentrations, tend to be, as expected, shorter at very short reaction time (5 min), passing trough a mixture of both shapes and becoming mostly infinitely long rods, at 10 min, and finally, being infinitely long when the hexagonal phase appears. Note also that the axial ratio for the ellipsoid form factor increases with time for all samples. The electron density of the corona region of the micelles also increases with time, which has been attributed to silicate-induced densification of the palisade layer[28,32] and concurrent expulsion of water.[45]

The salts also seem to have an influence on the radius of the hydrophobic core and the thickness of the micellar corona. In the no salt sample, the core radius ($R_{cor}$) and the corona thickness are both 31 Å. With the addition of NaCl, $R_{cor}$ increases and the corona thickness decreases (see Table 1). Addition of NaBr, on the other hand, does not show a continuous variation. With the addition of 1.0 M NaBr, $R_{cor}$ = 32 Å and corona thickness = 31 Å, which is the same as for the no salt sample. Complementary investigations were also made with 0.5 and 1.5 M NaBr. However, these mesurements, done during a second beamtime, suffered from lower signal-to-noise ratio. Therefore, these results will be shown just to check the trends and as a comparison with the 1.0 M NaBr results. The fitting results of these two concentrations indicate a decrease of $R_{cor}$ (25 and 26 Å, respectively) and an increase in the corona thickness (33 and 34 Å, respectively). We can thus expect that NaBr does not lead to an increase of the core radius, nor to a decrease of the corona thickness.

The general trend of increasing the hydrophobic core radius and decreasing the thickness of the corona layer with increasing NaCl concentrations can be attributed to the fact that $Cl^-$ ions are depleted from the corona region (EO units), causing a dehydration at this location.[15,46] The increase in hydrophobicity tends to increase the aggregation number of the micelles; hence, the core will increase in size, as expected.[47,48]

The overall effect of NaBr was different as compared to NaCl, as the diameter of the micelles remained unchanged or even seemed to decrease slightly in the presence of NaBr as compared to the "no salt" case, while the opposite was observed for NaCl. Figure S9 in Supporting Information shows the experimental curve of the sample without salt at 10 min into the reaction together with the form factors of infinite cylinders with $R_{cor}$ equal to 26 and 34 Å, corresponding to the values obtained from the fittings to 1.5 NaBr and 0.5 and 1.0 M NaCl, respectively, showing that neither bigger nor smaller radii correspond to the micelles present in the sample without salt. The promoted hydration of the EO groups in the palisade layer also allows the silicate units to travel deeper into it in the presence of NaBr. Note that this is the case even if all sols, including the NaBr and NaI containing sols, have a 1.6 M background concentration of $Cl^-$ ions.

As the scattering length for NaI micelles was too low compared to the solvent, the SAXS data could not be fitted. Even so, some information can be inferred from the NaI containing syntheses. In Figure 5, the times where phase separation is visually detected (i.e., when the sols are turbid) are plotted against the concentration for the three salts. The general trend in the data is that increasing salt concentrations leads to a faster phase separation. Moreover, the effect follows the order $Cl^-$ > $Br^-$ > $I^-$, i.e., that of the Hofmeister series. Thus, although no analysis of the micellar scattering region could be performed for NaI containing sols, the effect of NaI is expected to decrease the diameter of hydrophobic core, and increase the corona thickness of the micelles, due to the stronger salting-in behavior of $I^-$ as compared to $Br^-$.

Figure 6 shows the time of appearance and the evolution of the cell parameter of the first (10) Bragg reflection (left column). This reflection can indeed be attributed to the (10) reflection of a 2D hexagonal phase, as higher-order reflections appear almost at the same time (see Figure 2 and Supporting Information Figure S1). In the "no salt" case, the (10) reflection appears 38 min after the reaction started (i.e., addition of TEOS), and the cell parameter is 127 Å (Table 1). The value of the cell parameter decreases gradually with time, and reaches a plateau of 118 Å at about 200 min. The cell parameter values are close to the micellar diameter of 124 Å calculated based on the micellar scattering, suggesting a fairly close-packed arrangement of micellar rods in the mesophase in this case. However, the coexistence of micelles not included into the ordered structure is evident from the


dx.doi.org/10.1021/la1043798 |*Langmuir* 2011, 27, 7121–7131

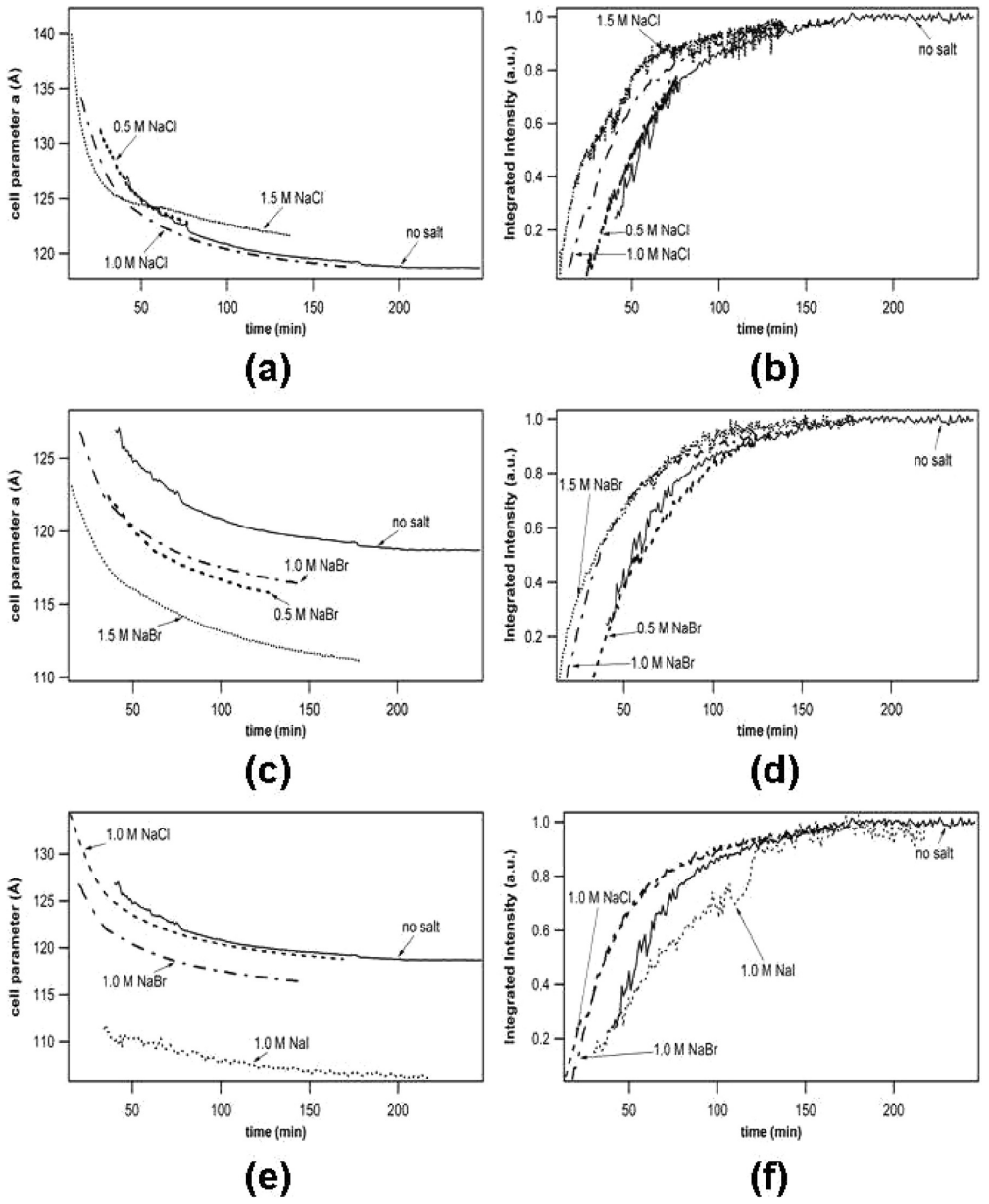


**Figure 6.** Left column: time evolution of cell parameter. Right column: time evolution of the integrated intensity, with plateau normalized to 1. (a,b). for NaCl; (c,d), for NaBr; (e,f), comparison of NaCl, NaBr, and NaI at 1.0 M.

presence of micellar scattering throughout the experimental observation time (see Figure 2a). The time of onset of mesophase formation (Figure 7) is shortened with increasing salt concentrations for both NaCl and NaBr, with NaCl giving the larger effect. When comparing the 1.0 M concentration of all the salts, the NaI synthesis is observed to have the smallest effect. The strength of influence thus follows the order $Cl^- > Br^- > I^-$.

Interestingly, as shown in Figure 6 (right column) the analysis of the evolution of the integrated intensity of the (10) reflection normalized to the last intensity reached in the experiment (which is very close to having reached a plateau) with time, shows that the kinetics of the growth process was almost identical in all cases, and followed first-order kinetics. A first-order kinetic process has also been observed for the early stage of mesophase formation in other related systems.[49,50] However, the nature of the anion has a strong influence on the initial value of the cell parameter, which increases with increasing NaCl concentration up to 140 Å for the sol containing 1.5 M NaCl, i.e., to values clearly exceeding the derived micellar diameters of about 120−128 Å. This immediately suggests that, in the flocs, the micelles, at this early stage of the mesophase formation process, are separated by a solvent layer, probably also containing some silicate species. However, the decrease of the value of the cell parameter with time is faster with increasing NaCl concentration, especially for sols containing 1.0 or 1.5 M NaCl, and similar plateau values as observed for the "no salt" case are reached at longer reaction times for sols containing up to 1.0 M NaCl, suggesting that the solvent layer is gradually squeezed out from the mesophase, in agreement with recent neutron scattering results.[45] For the sol containing 1.5 M NaCl, it seems that the plateau value is slightly higher than for sols containing lower NaCl concentrations, but the difference is quite small, just 2 Å


dx.doi.org/10.1021/la1043798 |*Langmuir* 2011, 27, 7121–7131

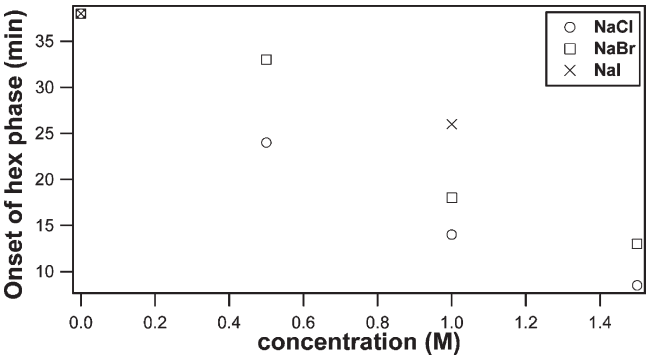


**Figure 7.** Time of onset of the mesophase, i.e., appearance of the Bragg reflection(s). Introducing salt decreases the initial lag time before the hexagonal phase appears. In the case of NaCl and NaBr, it is clear that the larger the concentration the stronger is the effect. It is also observed that NaCl has a larger effect than NaBr and that NaI (as shown for the 1.0 M concentration) has the smallest effect.

approximately; thus, we will not draw any lengthy conclusions about possible reasons for these differences based on the present set of data.

Surprisingly, the value of the cell parameter at a given point in time decreased with increasing salt concentration for sols containing NaBr as compared to the "no salt" case. Plateau values close to 110 Å were reached at higher salt concentrations and longer reaction times. This is close to the cell parameters determined for all studied materials after aging at 90 °C and subsequent drying (results not shown), so it is clear that NaBr promotes the formation of very compact structures already during the early stages of formation of the 2D hexagonal phase. Thus, if the micellar scattering analysis is linked with the analysis of the cell parameter values, it appears that salting-in anions promote a penetration of silicate species deeper into the palisade layer, which is reflected in the early formation of more compact hexagonal phases. This is qualitatively true for NaI, although micellar scattering analysis could not be carried out. Even more compact structures were observed for 1 M NaI as compared to 1 M NaBr (see Figure 6e), in accordance with the Hofmeister series.

The scanning electron micrographs shown in Figure 8 demonstrate the effect that the dynamics of formation has on the particle size and morphology. The particles were synthesized without salt and with 1.0 M of the respective salts. The most well-defined and smallest particles (on average 1.2 $\mu$m; Figure 8b) are found in the synthesis with the fastest formation kinetics (with 1.0 NaCl), in agreement with a process based on formation of a large number of nuclei. The 1 M NaBr synthesis produces particles with an average particle size of 3.7 $\mu$m with slightly less well-defined morphology (Figure 8b). In the no-salt case, the average particle size is about 2.7 $\mu$m, but the particle size distribution appears broader (Figure 8a), whereas for the NaI containing synthesis, the product consists of undefined pieces of material (Figure 8d). It is clear that salt additions have a critical effect on the nucleation and growth, which could be used, in this respect, as a controlling tool in the synthesis.

## DISCUSSION

Addition of ions to an aqueous solution of an EO-containing substance causes a general ion effect whereby the solubility of the

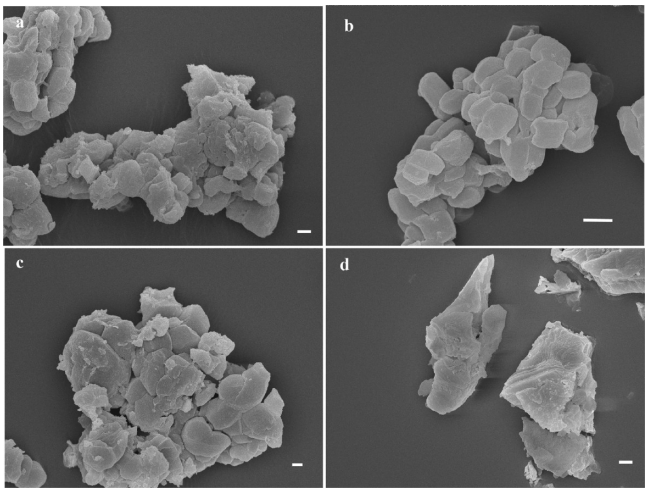


**Figure 8.** Scanning electron micrographs of (a) no-salt synthesis, (b) 1.0 M NaCl synthesis, (c) 1.0 M NaBr synthesis, and (d) 1.0 M NaI synthesis. Scale bars are 1 $\mu$m. The most well-defined particles are obtained in the NaCl-containing synthesis, followed by the NaBr-containing synthesis. Addition of NaI gives particles with undefined morphology. The particle size and size distribution vary. Addition of NaCl gives the smallest particles (approx 1 $\mu$m), NaBr gives slightly larger particles, and in the no salt case, the size variation is larger and the particle morphology less clear.

EO groups[51] decreases as the polarity of the solution increases. Kabalnov et al.[15] explained this phenomenon as stemming from an osmotic effect caused by ions being depleted from the EO part, thus generating dehydration of this part. This dehydration effect has been experimentally observed for different nonionic surfactants[15,52] including Pluronics[47] mainly by a decrease in the critical micellar concentration (cmc) and the cloud point[53] but also increasing the aggregation number of the micelles.[47,48] Jain et al.[47] showed that increasing the KCl concentration of a micellar Pluronic block copolymer solution increased the aggregation number of the micelles from 72 (no salt added) to 141 at 2.0 M KCl with a concomitant increase in the micellar radius. This effect can, however, be counterbalanced by a specific ion effect whereby certain ions adhere to the EO groups. Large polarizable anions like $I^-$ are known to adhere to EO groups.[12,15] According to the Hofmeister series, the salting-in (i.e., absorption in the EO part) to the salting-out (depletion from the EO part) order of the anions in this study is the following: $I^-$, $Br^-$, and $Cl^-$. We would expect all salts to contribute to the general ion effect, but this effect is counterbalanced by the specific ion effect, which is expected (following the Hofmeister series) to be stronger for NaI than for NaBr. In this work, we can identify two phenomena resulting from the general and specific ion effect. The first that will be considered is the influence on the size of the micelles, which, in turn, affects the cell parameter of the mesoscopic structure. The other is the effect on the dynamics of the process.

The general ion effect is apparent by examining, for instance, the core radius of the micelles 5 min into the reaction for the concentration series with NaCl. The core radius increases almost linearly from 31 Å for the no-salt synthesis to 38 Å for the 1.5 M NaCl containing synthesis, in accordance with the results obtained by Jain et al.[47] This is reflected in the values of the initial cell parameter of the hexagonal phase obtained for the NaCl


dx.doi.org/10.1021/la1043798 |*Langmuir* 2011, 27, 7121–7131

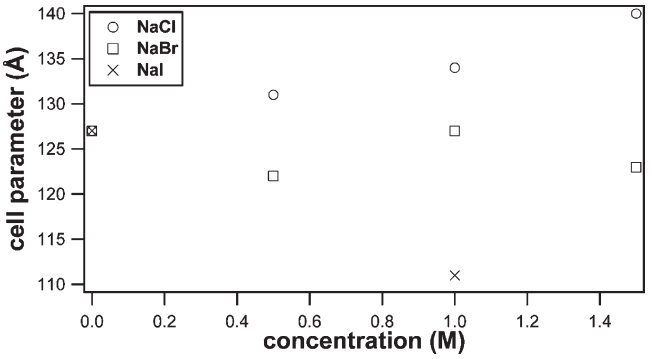


**Figure 9.** Initial cell parameter for the synthesis studied (NaCl and NaBr at 0.5 M, 1.0, and 1.5 M, and NaI at 1.0 M concentration along with the synthesis performed with no salt).

containing syntheses shown in Figure 9. It is clear that an increase in salt concentration leads to an increase in the initial cell parameter. The cell parameter increases from 127 Å for the synthesis without salt to 140 Å for the 1.5 M NaCl containing synthesis. Taking into consideration the specific salt effect, based on the discussion above, the core radius, as well as the initial cell parameter, should, for each salt concentration, show a lower value for NaBr and an even lower value for NaI, demonstrating the stronger counterbalancing effect of $I^-$ than $Br^-$. This is indeed what is observed (cf. Figure 9 and Table 1). It is also suggested that the salting-in behavior allows silica solution to penetrate deeper into the micellar core, which swiftly leads to a more compact structure (cf. Figure 6). Notice that, for 0.5 M NaBr, the initial cell parameter is lower than the total micellar radius. In the case of this sample, it was impossible to have a reasonable fitting result for smaller radius. Although its core radius is very small, the corona is very thick; thus, the EO groups became hydrophilic enough to have enough water and silica in it.

The other effect of the difference in salting-in/out behavior of the salts is apparent by considering the dynamics of the mesophase formation. Figures 5 and 7 show the time of phase separation and the time when the mesophase first appears, i.e., when the (10) reflection first becomes visible. All the salts induce faster dynamics, and the effect is larger with increasing concentration. It is also clear that the phase separation occurs prior to the hexagonal phase in accordance with our previous study,[30] although the times are obviously less accurately determined than the appearance of the mesophase. Even so, the trends are the same in both investigations. The specific ion effect is perceived by examining the three salts at equivalent concentrations. This holds for each concentration. As expected, formation of the mesophase (and phase separation) is slower for the NaI-containing syntheses. Syntheses made in the presence of NaCl show the fastest behavior. NaBr containing syntheses have an intermediate behavior. Hence, in this respect also the order follows the Hofmeister series. The particle size and morphology (Figure 8) is in accordance with this, as the NaCl system results in the smallest, most well-defined particles (fast nucleation provides many and small particles).

In order to clarify whether the salts have an influence only on the micellar properties or the silica polymerization is also affected, we examined the silica condensation kinetics, as judged by visual determination of the gel formation of the corresponding sols in the absence of surfactant. The times of gel formation were almost identical for all sols containing sodium salt and only slightly shorter for the sol without added salt. This shows that the salt additions primarily influence the micellar properties rather then silica kinetics. On the basis of this argument, we can thus assume that the siliceous species at the onset of the mesophase formation are less developed or interconnected for a fast (e.g., NaCl containing process) process than for a slow one. Further, it is expected that more water will be present in the floc for the faster processes. Hence, the value of the cell parameter for the mesophase should decrease more for a fast process as a consequence of water being expelled. In a recent small angle neutron scattering study, the water expulsion from SBA-15 was monitored in situ.[51] It was shown that more water is expelled when salt is present in the synthesis. In this study, it is clear that the cell parameter value has a larger decrease when salt, in particular, NaCl, is present. The structure, at the onset of formation, would, as a consequence of this, be more flexible, allowing more molecular rearrangement and therefore a better chance of reaching a thermodynamically stable structure. Hence, the more aqueous environment and the less condensed silica species enable more flexibility during the formation process, providing means for the development of a more ideal structure with straight, or less corrugated, pores. The improved structural properties for the NaBr and, in particular, for the NaCl containing synthesis is apparent in Figure 2 where the higher-order reflections are present in the salt containing syntheses. In addition, the form factor oscillations caused by the micellar scattering disappear quickly in the salt syntheses, whereas it persists in the no-salt case until the end of the measurement.

The shorter time needed for the formation of the mesophase, as well as the presence of higher-order reflections for the samples containing NaCl and NaBr, clearly indicate that the salts promote the mesophase formation kinetics. This structural promoting effect has also been observed in the final mesoporous materials synthesized under the presence of NaCl,[3] as well as the shorter precipitation time found by Zhao et al. in the presence of different anions,[1,54] finding, like us, similar mesophase formation times for $Br^-$ and $Cl^-$, both shorter than for the other studied anions. It is also clear that electrolytes can be used as a tool for controlling particle size.

## CONCLUSION

The presence of salt in the synthesis of SBA-15 speeds up the dynamics of mesophase formation. It also influences the micellar core/corona properties which have an influence on the cell parameters of the SBA-15 structure. Our observations show that the anions studied follow the Hofmeister series with $Cl^-$ having the largest effect, followed by $Br^-$ and with $I^-$ having the smallest impact. It was also seen that with increasing concentration the effect increased. Faster dynamics provides the means for a more flexible route to the final mesostructure, which resulted in improved order (demonstrated by the number of reflections and the absence of micellar scattering once the mesostructure is formed) of the material. Further, it is expected that a flexible formation route, as in the NaCl case, would provide the means for obtaining less corrugated pores. However, for the properties regarding the porosity of the final material, the subsequent steps (hydrothermal treatment and calcination) could have a major influence. This issue is the focus of a study currently underway.

## ASSOCIATED CONTENT

**Supporting Information.** Time-resolved SAXS patterns for synthesis containing NaCl and NaBr at 0.5 and 1.5 M (S1).

Scattering curves in log scale for no salt and 1.0 M NaCl (S2−S3). Scattering curves for syntheses at different times and different conditions with fitted form factors (S4−S8). Scattering curve of no salt sample along with modeled form factors with different radius (S9). This material is available free of charge via the Internet at http://pubs.acs.org.

## AUTHOR INFORMATION


### Corresponding Author

*E-mail: Viveka.Alfredsson@fkem1.lu.se.

### Present Addresses

[#]Instituto de Física, Universidade Federal do Rio Grande do Sul, Caixa Postal 15051, CEP 91501−970, Porto Alegre, RS, Brazil.


## ACKNOWLEDGMENT

Håkan Wennerström is acknowledged for insightful discussions. Financial support came from the Swedish Research Council partly via the Linnaeus Centre of Excellence, Organizing Molecular Matter (V.A.), from the SSF program COLINTECH (P.L.), Ministry of Science and Innovation of Spain (subprogram RYC-2005-001625 and project MAT 2008-01080/MAT) (C.V.T) and Generalitat de Catalunya (project EME2007-11) (C.V.T.). Tomas Kjellman is acknowledged for performing the scanning electron microscopy measurements.

## REFERENCES


(1) Zhao, D.; Huo, Q.; Feng, J.; Chmelka, B. F.; Stucky, G. D. *J. Am. Chem. Soc.* **1998**, *120*, 6024.

(2) Zhao, D.; Yang, P.; Chmelka, B. F.; Stucky, G. D. *Chem. Mater.* **1999**, *11*, 1174.

(3) Wang, Y. Q.; Yang, C. M.; Zibrowius, B.; Spliethoff, B.; Lindén, M.; Schüth, F. *Chem. Mater.* **2003**, *15*, 5029.

(4) Tang, J.; Yu, C.; Zhou, X.; X., Y.; Zhao, D. *Chem. Commun.* **2004**, *2004*, 2240.

(5) Lin, H.-P.; Kao, C.-P.; Mou, C.-Y.; Liu, S.-B. *J. Phys. Chem. B* **2000**, *104*, 7885.

(6) Lin, H.-P.; Mou, C.-Y. *Microporous Mesoporous Mater.* **2002**, *55*, 69.

(7) Flodström, K.; Alfredsson, V.; Källrot, N. *J. Am. Chem. Soc.* **2003**, *125*, 4402.

(8) Wang, L.; Qi, T.; Zhang, Y.; Chu, J. *Microporous Mesoporous Mater.* **2006**, *91*, 156.

(9) Kubo, S.; Kosuge, K. *Langmuir* **2007**, *23*, 11761.

(10) Jönsson, B.; Lindman, B.; Holmberg, K.; Kronberg, B. *Surfactants and Polymers in Aqueous Solution*; John Wiley & Sons Ltd.: New York, 1998.

(11) Mortensen, K. *Polymers Adv. Technol.* **2001**, *12*, 2.

(12) Alexandridis, P.; Holzwarth, J. F. *Langmuir* **1997**, *13*, 6074.

(13) Ivanova, R.; Lindman, B.; Alexandridis, P. *Langmuir* **2000**, *16*, 3660.

(14) Wanka, G.; Hoffmann, H.; Ulbricht, W. *Macromolecules* **1994**, *27*, 4145.

(15) Kabalnov, A.; Olsson, U.; Wennerström, H. *J. Phys. Chem.* **1995**, *99*, 6220.

(16) Leontidis, E. *Curr. Opin. Colloid Interface Sci.* **2002**, *7*, 81.

(17) Kleitz, F.; Choi, S. H.; Ryoo, R. *Chem. Commun.* **2003**, 2136.

(18) Flodström, K.; Alfredsson, V. *Microporous Mesoporous Mater.* **2003**, *59*, 167.

(19) Yu, C.; Tian, B.; Fan, J.; Stucky, G. D.; Zhao, D. *Chem. Commun.* **2001**, 2726.

(20) Ruthstein, S.; Raitsimrig, A. M.; Bitton, R.; Frydman, V.; Godt, A.; Goldfarb, D. *Phys. Chem. Chem. Phys.* **2009**, *11*, 148.

(21) Ruthstein, S.; Frydman, V.; Kababya, S.; Landau, M.; Goldfarb, D. *J. Phys. Chem. B* **2003**, *107*, 1739.

(22) Ruthstein, S.; Frydman, V.; Goldfarb, D. *J. Phys. Chem. B* **2004**, *108*, 9016.

(23) Ruthstein, S.; Schmidt, J.; Kesselman, E.; Talmon, Y.; Goldfarb, D. *J. Am. Chem. Soc.* **2006**, *128*, 3366.

(24) Flodström, K.; Wennerström, H.; Alfredsson, V. *Langmuir* **2004**, *20*, 680.

(25) Sierra, L.; Valange, S.; Guth, J.-L. *Microporous Mesoporous Mater.* **2009**, *124*, 100.

(26) Mesa, M.; Sierra, L.; Guth, J.-L. *Microporous Mesoporous Mater.* **2008**, *112*, 338.

(27) Sundblom, A.; Palmqvist, A. E. C.; Holmberg, K. *Langmuir* **2010**, *26*, 1983.

(28) Flodström, K.; Teixeira, C. V.; Amenitsch, H.; Alfredsson, V.; Lindén, M. *Langmuir* **2004**, *20*, 4885.

(29) Flodström, K.; Wennerström, H.; Teixeira, C. V.; Amenitsch, H.; Lindén, M.; Alfredsson, V. *Langmuir* **2004**, *20*, 10311.

(30) Linton, P.; Rennie, A. R.; Zackrisson, M.; Alfredsson, V. *Langmuir* **2009**, *25*, 4685.

(31) Sundblom, A.; Oliveira, C. L. P.; Palmqvist, A. E. C.; Pedersen, J. S. *J. Phys. Chem. C* **2009**, *113*, 7706.

(32) Khodakov, A. Y.; Zholobenko, V. L.; Imperor-Clerc, M.; Durand, D. *J. Phys. Chem. B.* **2005**, *109*, 22780.

(33) Zholobenko, V. L.; Khodakov, A. Y.; Impéror-Clerc, M.; Durand, D.; Grillo, I. *Adv. Colloid Interface Sci.* **2008**, *142*, 67.

(34) Linton, P.; Alfredsson, V. *Chem. Mater.* **2008**, *20*, 2878.

(35) Sundblom, A.; Oliveira, C. L. P.; Pedersen, J. S.; Palmqvist, A. E. C. *J. Phys. Chem. C* **2010**, *114*, 3483.

(36) Linton, P.; Hernandez-Garrido, J.-C.; Midgley, P.; Wennerström, H.; Alfredsson, V. *Phys. Chem. Chem. Phys.* **2009**, *11*, 10973.

(37) Schmidt-Winkel, P.; Yang, P.; Margolese, D. I.; Chmelka, B. F.; Stucky, G. D. *Adv. Mater.* **1999**, *11*, 303.

(38) Linton, P.; Wennerstroem, H.; Alfredsson, V. *Phys. Chem. Chem. Phys.* **2010**, *12*, 3852.

(39) Baute, D.; Goldfarb, D. *J. Phys. Chem. C* **2007**, *111*, 10931.

(40) Ågren, P.; Lindén, M.; Rosenholm, J.; Schwarzenbacher, R.; Kriechbaum, M.; Amenitsch, H.; Laggner, P.; Blanchard, J.; Schüth, F. *J. Phys. Chem. B* **1999**, *103*, 5943.

(41) Amenitsch, H.; Rappolt, M.; Kriechbaum, M.; Mio, H.; Laggner, P.; Bernstorff, S. *J. Synchrotron Radiat.* **1998**, *5*, 506.

(42) Marignan, J.; Basserau, P.; Delord, P. *J. Phys. Chem. B* **1986**, 90.

(43) Glatter, O.; Kratky, O. *Small-angle x-ray scattering*; Academic Press: London, 1982.

(44) Boissière, C.; Larbot, A.; Bourgaux, C.; Prouzet, E.; Bunton, C. A. *Chem. Mater.* **2001**, *13*, 3580.

(45) Linton, P.; Rennie, A. R.; Alfredsson, V. *J. Solid State Sci.* **2011**, *13*, 793.

(46) Kalra, A.; Tugcu, A. N.; Cramer, M.; Garde, S. *J. Phys. Chem. B* **2001**, *105*, 6380.

(47) Jain, N. J.; Aswal, V. K.; Goyal, P. S.; Bahadur, P. *Colloids Surf., A* **2000**, *173*, 85.

(48) Galarneau, A.; Cambon, H.; Di Renzo, F.; Ryoo, R.; Choi, M.; Fajula, F. *New J. Chem.* **2003**, *27*, 73.

(49) Beurroies, I.; Ågren, P.; Büchel, G. R., J. B.; Amenitsch, H.; Denoyel, R.; Linden, M. *J. Phys. Chem. B* **2006**, *110*, 16254.

(50) Né, F.; Testard, F.; Zemb, T.; Grillo, I. *Langmuir* **2003**, *19*, 8503.

(51) Shusharina, N. P.; Baliepalli, S.; Gruenbauer, H. J. M.; Alexandridis, P. *Langmuir* **2003**, *19*, 4483.

(52) Iwanaga, T.; Suzuki, M.; Kunieda, H. *Langmuir* **1998**, *14*, 5775.

(53) Alexandridis, P.; Olsson, U.; Lindman, B. *Langmuir* **1997**, *13*, 23.

(54) Zhao, D.; Feng, J.; Huo, Q.; Melosh, N.; Fredrickson, G. H.; Chmelka, B. F.; Stucky, G. D. *Science* **1998**, *279*, 548.